

Quantitative Analysis of Light-Harvesting Efficiency and Electron-Transfer Yield in Ruthenium-Dye-Sensitized Nanocrystalline TiO_2 Solar Cells

Yasuhiro Tachibana,* Kohjiro Hara, Kazuhiro Sayama, and Hironori Arakawa*

Photoreaction Control Research Centre (PCRC), National Institute of Advanced Industrial Science and Technology (AIST), 1-1-1, Higashi, Tsukuba, Ibaraki 305-8565, Japan

Received November 9, 2001. Revised Manuscript Received April 2, 2002

We have conducted a quantitative analysis of light-harvesting efficiency and electron-transfer yield for solar cells employing ruthenium dye, $(\text{tetrabutylammonium})_2 \text{cis-}(2,2'\text{-bipyridyl-4-COOH, 4'-COO})_2(\text{NCS})_2$ ruthenium(II), sensitized nanocrystalline TiO_2 films with a series of light-scattering magnitudes. The light-harvesting efficiency increases with the addition of relatively large particles to a transparent film, especially for near-infrared wavelengths. Excess addition, however, lowers the light-harvesting efficiency over the whole visible wavelengths owing to enhanced light reflection at the conducting glass/ TiO_2 interface. Following a rigorous calculation using the results obtained from the light-harvesting efficiency and the short-circuit photocurrent measurements, we demonstrate for the first time that the electron-transfer yield markedly decreases with increasing optical thickness, that is, film light-scattering magnitude, by a maximum of $\approx 60\%$. The origins of the change in the electron-transfer yield can be complex, involving multiple excitation or many electron-transfer processes. The analytical results obtained in this study suggest that an appropriate light-scattering magnitude in the TiO_2 film originating from particle sizes, their distribution, and the film thickness is a key parameter in controlling the electron-transfer yield as well as the light-harvesting efficiency and thus the short-circuit photocurrent.

Introduction

Photovoltaics based upon nanocrystalline semiconductor sensitized by dyes are of great interest in alternative solar energy conversion devices compared to the conventional Si or GaAs cells.^{1,2} This novel cell employs simple chemical substances, such as titanium dioxide and organic dyes, and claims not only commercial application for new energy sources but also scientific interest to understand its mechanism. The main attention to date has been focused upon the high solar-to-electric conversion efficiency for a cell employing a nanocrystalline TiO_2 film sensitized by a ruthenium complex.^{3,4} For example, combination of a TiO_2 film and $[(\text{C}_4\text{H}_9)_4\text{N}]_3\text{Ru}(\text{Htctery})(\text{NCS})_3$ (tctery = 4,4',4''-tricarboxy-2,2':6',2''-terpyridine), that is, black dye, has achieved an efficiency of $< 11\%$.^{5,6}

The cell performance, that is, solar-to-electric conversion efficiency, is determined by the short-circuit photocurrent (J_{sc}), open-circuit photovoltage (V_{oc}), and fill factor (ff) under a definite intensity of light such as the AM1.5 solar spectrum. J_{sc} can be increased by raising the light-harvesting efficiency (LHE), that is, light absorbance by the dye-sensitized TiO_2 film. For the cell employing sensitizer dye, $\text{cis-}(2,2'\text{-bipyridyl-4,4'-dicarboxylate})_2(\text{NCS})_2$ ruthenium(II), an incident photon-to-current conversion efficiency (IPCE) was near unity in the 400–550-nm wavelength range,⁴ which in turn indicates that the LHE is also near unity in the same wavelength range. However, light absorption greater than 600 nm remains poor, although the roughness factor, defined as the ratio of the real to the projected surface of the film,⁶ is greatly enhanced within the nanocrystalline TiO_2 film to increase the concentration of the dye adsorbed.

According to the Lambert–Beer law, the cell's LHE is determined by the dye extinction coefficient, the attached dye concentration, and the optical path length within the film. Improvement of the LHE is dependent upon whether the appropriate dye absorbance can be extended to a wider wavelength range, especially for wavelengths > 700 nm. Intensive studies have been conducted to investigate sensitizer dyes with wide light absorption bands^{7,8} or sensitizer dye blends.⁹ When the

* To whom correspondence should be addressed. E-mail: yasu.tachibana@aist.go.jp. Fax: 00-81-(0)298-61-4750.

(1) Markvart, T. *Solar Electricity*; John Wiley & Sons: New York, 2000.

(2) Partain, L. D. *Solar Cells and Their Applications*; John Wiley & Sons: New York, 1995.

(3) O'Regan, B.; Moser, J. E.; Anderson, M.; Grätzel, M. *J. Phys. Chem.* **1990**, *94*, 8720–8726.

(4) Nazeeruddin, M. K.; Kay, A.; Rodicio, I.; Humphry-Baker, R.; Muller, E.; Liska, P.; Vlachopoulos, N.; Grätzel, M. *J. Am. Chem. Soc.* **1993**, *115* (14), 6382–6390.

(5) Nazeeruddin, M. K.; Péchy, P.; Renouard, T.; Zakeeruddin, S. M.; Humphry-Baker, R.; Comte, P.; Liska, P.; Cevey, L.; Costa, E.; Shklover, V.; Spiccia, L.; Deacon, G. B.; Bignozzi, C. A.; Grätzel, M. *J. Am. Chem. Soc.* **2001**, *123*, 1613–1624.

(6) Kalyanasundaram, K.; Grätzel, M. *Coord. Chem. Rev.* **1998**, *77*, 347–414.

(7) Hara, K.; Sayama, K.; Ohga, Y.; Shinpo, A.; Suga, S.; Arakawa, H. *Chem. Commun.* **2001**, 569–570.

(8) Nazeeruddin, M. K. Personal communications.

same sensitizer dye is used, the LHE can be further enhanced by increasing the attached dye concentration or the optical path length by modification of nanocrystalline TiO_2 films. The attached dye concentration is dominated by the surface area enhanced by decreasing the particle size (down to 10–20 nm in diameter). Further decrease is difficult because such a size decrease is not suitable for colloid synthesis and screen-printing film preparation. Studies have then been focused upon increasing the film optical length achieved by the addition of relatively large particles into a small particle solution to induce light scattering within the TiO_2 film, and J_{sc} improvement was indeed observed.^{5,10}

The light-scattering property of TiO_2 films induced by introducing relatively large particles into small particles has been simulated theoretically, using a multiflux model¹¹ or radiative transport theory.¹² Ferber and Luther calculated the optimum size and ratio of large particles mixed with small particles (20 nm in diameter)¹² and predicted the maximum LHE of the dye-sensitized TiO_2 film. They also concluded that the excess of the large particles enhances front surface light reflection, resulting in a LHE decrease. Rothenberger et al. employed a four-flux model to explain the light-scattering properties and concluded that an appropriate mixture of small and large particles synthesized from acidic and basic TiO_2 solution, respectively, exhibits the maximum LHE over wavelengths considered for light absorption.¹¹ It is thus of great importance to correlate these theoretical results with experimental data because this could indicate the key parameters involved in controlling the J_{sc} .

J_{sc} can be calculated by integrating the product of the incident photon flux density and the cell's IPCE over wavelengths used for light absorption by the dye. According to the equation used to describe the J_{sc} for the photovoltaic cells,² with the assumption that the potential drop by series resistance in the cell is negligible, the J_{sc} is shown as follows,

$$J_{\text{sc}} = \int qF(\lambda)[1 - r(\lambda)]\text{IPCE}(\lambda) \, d\lambda \quad (1)$$

where q is the electron charge, $F(\lambda)$ is the incident photon flux density at wavelength λ , and $r(\lambda)$ is the incident light loss before reaching the TiO_2 film in the cell, for example, the reflection loss at interfaces. The IPCE is expressed⁴ as

$$\text{IPCE}(\lambda) = \text{LHE}(\lambda)\phi_{\text{e-inj}}\eta_{\text{ChargeCollection}} = \text{LHE}(\lambda)\Phi(\lambda)_{\text{ET}} \quad (2)$$

where $\phi_{\text{e-inj}}$ is the electron injection yield from the dye excited state into TiO_2 , $\eta_{\text{ChargeCollection}}$ is the charge collection efficiency at the back SnO_2 electrode, and $\Phi(\lambda)_{\text{ET}}$ is defined as an electron-transfer yield, that is, a product of the electron injection yield and the charge collection efficiency. This electron-transfer yield is also

expressed as an absorbed photon-to-current conversion efficiency (APCE). From eqs 1 and 2, the relationship between the J_{sc} and the LHE can be expressed as follows:

$$J_{\text{sc}} = \int qF(\lambda)[1 - r(\lambda)]\text{LHE}(\lambda)\Phi(\lambda)_{\text{ET}} \, d\lambda \quad (3)$$

When $\Phi(\lambda)_{\text{ET}}$ is averaged over the wavelengths probed, the average electron-transfer yield term, Φ_{ET} , can be taken out of the integral. The equation is therefore simplified to

$$J_{\text{sc}} = \Phi_{\text{ET}} \int qF(\lambda)[1 - r(\lambda)]\text{LHE}(\lambda) \, d\lambda \quad (4)$$

Because we are able to observe LHE, $r(\lambda)$, $F(\lambda)$, and J_{sc} , the average electron-transfer yield can be calculated using eq 4 for any cell based upon dye-sensitized TiO_2 films.

Several groups have studied forward kinetic processes in the cell, such as electron injection from the dye excited state into TiO_2 ,^{13–15} electron transport within TiO_2 films,^{16–18} dye regeneration by the redox electrolyte,^{19,20} and electrolyte mass transport.²¹ As for reverse electron-transfer reaction processes, charge recombination between the electron in the TiO_2 and the oxidized dye^{22,23} or the oxidized electrolyte²⁴ was also reported. However, these experiments were mainly carried out with transparent TiO_2 films because they are most suitable for kinetic experiments by means of optical and electro-optical spectroscopies.

Little attention has been paid to the influence of light scattering on the electron-transfer kinetics in the dye-sensitized TiO_2 films because quantitative measurements of the electron-transfer kinetics have been limited, owing to the difficulty in observing photons emitted from the scattered TiO_2 film. A reasonable assumption follows that the highly scattered TiO_2 films exhibit identical kinetics as transparent films. However, the electron-transfer rates may be influenced by local dye excitation within the scattered film. For example, photons exposed to the scattered film might travel in the same path coherently or incoherently, resulting in inhomogeneous excitation magnitude throughout the film. Such excitation may change the local concentrations of the dye excited states and the charge-separated states and in turn influence the electron injection

(13) Tachibana, Y.; Moser, J. E.; Grätzel, M.; Klug, D. R.; Durrant, J. R. *J. Phys. Chem.* **1996**, *100*, 20056–20062.

(14) Ellingson, R. J.; Asbury, J. B.; Ferrere, S.; Ghosh, H. N.; Sprague, J.; Lian, T.; Nozik, A. J. *J. Phys. Chem. B* **1998**, *102*, 6455–6458.

(15) Hannappel, T.; Burfeindt, B.; Storck, W.; Willig, F. *J. Phys. Chem. B* **1997**, *101*, 6799–6802.

(16) Vanmaekelbergh, D.; de Jongh, P. E. *J. Phys. Chem. B* **1999**, *103*, 747–750.

(17) van de Lagemaat, J.; Park, N. G.; Frank, A. J. *J. Phys. Chem. B* **2000**, *104*, 2044–2052.

(18) Dloczik, L.; Ileperuma, O.; Lauermann, I.; Peter, L. M.; Ponomarev, E. A.; Redmond, G.; Shaw, N. J.; Uhlendorf, I. *J. Phys. Chem. B* **1997**, *101*, 10281–10289.

(19) Haque, S. A.; Tachibana, Y.; Klug, D. R.; Durrant, J. R. *J. Phys. Chem. B* **1998**, *102*, 1745–1749.

(20) Pelet, S.; Moser, J. E.; Grätzel, M. *J. Phys. Chem. B* **2000**, *104*, 1791–1795.

(21) Papageorgiou, N.; Barbe, C.; Grätzel, M. *J. Phys. Chem. B* **1998**, *102*, 4156–4164.

(22) Hagfeldt, A.; Grätzel, M. *Chem. Rev.* **1995**, *95*, 49–68.

(23) Haque, S. A.; Tachibana, Y.; Willis, R.; Moser, J. E.; Grätzel, M.; Klug, D. R.; Durrant, J. R. *J. Phys. Chem. B* **2000**, *104*, 538–547.

(24) Schlichthorl, G.; Huang, S. Y.; Sprague, J.; Frank, A. J. *J. Phys. Chem. B* **1997**, *101*, 8141–8155.

(9) Alonso, N. V.; Beley, M.; Chartier, P. *Rev. Phys. Appl.* **1981**, *16*, 5–10.

(10) Barbe, C. J.; Arendse, F.; Comte, P.; Jirousek, M.; Lenzmann, F.; Shklover, V.; Grätzel, M. *J. Am. Ceram. Soc.* **1997**, *80*, 3157–3171.

(11) Rothenberger, G.; Comte, P.; Grätzel, M. *Sol. Energy Mater. Sol. Cells* **1999**, *58*, 321–336.

(12) Ferber, J.; Luther, J. *Sol. Energy Mater. Sol. Cells* **1998**, *54*, 265–275.

Table 1. Characteristics of TiO_2 Films with a Series of Light-Scattering Magnitude (Listed from Transparent to Scattering)

type of TiO_2 particles used to prepare nanocrystalline films ^a	porosity	roughness factor (10- μ m-thick film)	average diameter (nm) ^b
film-1: synthesized in acidic solution	0.66	1450	14.0
film-2: commercial (Ishihara, ST2-02)	0.58	1650	15.2
film-3: synthesized in acidic and basic solutions	0.55	1160	23.3
film-4: commercial (Nippon aerosil, P-25)	0.73	640	24.9
film-5: synthesized in acidic and basic solutions	0.59	1090	22.3
film-6: synthesized in basic solution	0.52	840	34.2
film-7: commercial (Furukawa, DN-S1)	0.74	1100	14.0
film-8: commercial (Ishihara, ST-01 & Wako)	0.61	630	37.5
film-9: commercial (Wako)	0.52	340	85.3

^aThe name of the commercial companies and the product names are shown in parentheses. ^bThe particle diameter was calculated from the surface area (measured by BET) and the film porosity. The particle size distribution was not considered, and therefore the data are averaged over mixed particles.

kinetics and the charge collection efficiency. Thus, it is necessary to address whether scattered light controls the electron-transfer kinetics in the dye-sensitized TiO_2 solar cell.

In this paper, we quantitatively conducted LHE measurements involving ruthenium-dye-sensitized TiO_2 films with a series of light-scattering magnitudes. The magnitude was varied by employing synthesized or commercial TiO_2 particles with different particle sizes. Absorbed and nonabsorbed photons by the sensitized film were quantitatively monitored by using a UV-vis steady-state absorption spectrometer with an integrating sphere detector. Following J_{sc} observation for the solar cells employing these TiO_2 films, the average electron-transfer yields consisting of the electron injection and the charge collection yields were calculated. These electron-transfer yields were further correlated with the light-scattering magnitude observed for the films. This indirect way to evaluate the electron-transfer yield shows a rather direct comparison of the parameters controlling the J_{sc} between the transparent and the scattered TiO_2 films.

Experimental Section

TiO₂ Film Preparation. Anatase TiO_2 colloids were either synthesized following the methods described in the literature^{10,25} or obtained from commercial sources (see Table 1). Preparation of a TiO_2 paste consisting of synthesized or commercial particles was carried out by modifying the method reported in the literature.⁵ Ethyl cellulose (Fluka) and α -terpineol (Kanto Chemicals, Japan) were added into the paste to obtain the appropriate viscosity for screen-printing. TiO_2 films were prepared by screen printing onto a fluorine-doped SnO_2 -coated glass (Nippon Sheet Glass, Japan, sheet resistance: 8–10 Ω/cm^2) for photoelectrochemical measurement or onto a thin cover glass (Matsunami, Japan, thickness: 0.17–0.25 mm) for LHE and light-scattering measurements. The film, after printing, was leveled for 15 min, heated to 500 °C at 33 °C/min, and calcined at 500 °C for 1 h in an air flow oven. The light-scattering magnitude in the film was controlled by an appropriate small and large particle size mixture. The film characteristics employed in the present study are summarized in Table 1. All films have an anatase form of TiO_2 except for film-4.

Sensitization of the film by the ruthenium dye, (tetrabutylammonium)₂ *cis*-(2,2'-bipyridyl-4-COOH, 4'-COO-)₂(NCS)₂-ruthenium(II): Ru(dcbpy)₂NCS₂ (Solaronix, Switzerland), was conducted by film immersion into the dye ethanol solution (0.3 mM) at room temperature overnight. Ru(dcbpy)₂NCS₂ was

chosen for the present study because this dye has to date been the most attractive for commercial application. Prior to sensitization, the films were treated with titanium tetrachloride solution to coat the surface with a thin TiO_2 layer using the previous method.⁵

Light-Scattering and LHE Measurements. The TiO_2 films employed in this study exhibited a series of light-scattering magnitudes, that is, from transparent to white in appearance. Scattered light emitted from the film travels in any random direction, depending upon the scattering magnitude. Complete photon collection is necessary to quantify the light absorption by the sensitized film. Incorporation of an integrating sphere into a UV-vis absorption spectrometer (Shimadzu, Japan, UV-3101PC) facilitates monitoring of the light from any direction. For data analysis, a two-flux model was employed, although a four-flux model is more commonly applied for the experimental data using a collimated beam in the spectrometer.¹¹ The advantage of employing the two-flux model is that the data are easily handled with simplified parameters to associate with the film characterization and the solar cell performance. The analyzed results showed a remarkable correlation between the film-scattering properties and the electron-transfer yield (see Discussion).

To characterize the light-scattering magnitude, the transmittance and reflectance were observed for unsensitized TiO_2 films. Figure 1 shows a sample configuration. TiO_2 was deposited on the thin glass plate and covered by methoxyacetonitrile, MeAN (>99% pure, Aldrich), and another thin glass plate. MeAN was employed in this study because it has been commonly accepted as the supporting electrolyte solvent in solar cells.¹⁰ A glass substrate was found to be critical for capturing all of the output light. For example, for a relatively thick substrate, scattered light leaks from the glass substrate side. A thin glass plate was therefore employed for the measurements. A sample was held at the entrance hole of the integrating sphere for the transmittance (forward side) measurement and at the exit hole for the reflectance (backward side) measurement. The sample was irradiated from behind the glass substrate on which the TiO_2 film is deposited. The incident angle is tilted by 8° from perpendicular to the sample face for the reflectance measurement to monitor the light reflection at the air/glass interface and reflectance from the TiO_2 film. The error for quantitative measurements within the integrating sphere is less than ±3%.

The LHE measurements were conducted with the same configuration as the light-scattering measurement. Identical TiO_2 films were used, but sensitized by the dye. The output light from the sample was monitored at the forward and backward sides (directions are shown in Figure 1). The light absorption ratio by the dye-sensitized TiO_2 film was obtained from the difference in the spectra between the sensitized and unsensitized films. The obtained spectra were corrected for light loss by reflection at the air/glass interface only to estimate light absorption by the dye-sensitized TiO_2 film without the glass substrate. Light absorption and/or reflection by the conducting glass were also measured by the integrating sphere detector to calculate the LHE of the film deposited on the

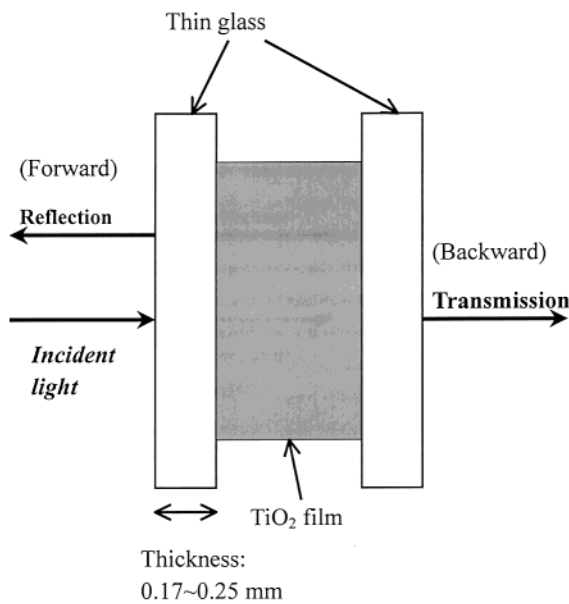


Figure 1. Illustration of the configuration employed to measure the UV-vis absorption spectrum with the integrating sphere. Photons emitted from the sample in the reflection (forward) or transmission (backward) direction were collected by the sphere detector.

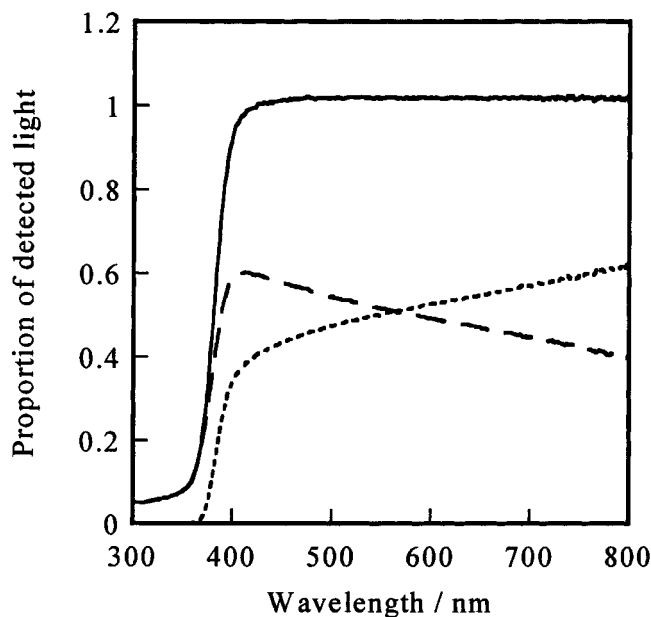


Figure 2. Transmission (dotted line: ...) and reflection (broken line: - - -) spectra emitted from the TiO₂ film after light irradiation. Solid line shows the addition of these spectra (—). The data are shown for film-5 (unsensitized).

conducting glass. Absorption by the electrolyte or the TiO₂ was not corrected to simplify the parameters.

Characterization of Light-Scattering Magnitude. The two-flux model was theoretically developed by Kubelka and Munk.^{26,27} TiO₂ is a white pigment; that is, no absorption of visible light is observed as shown in Figure 2. Under this condition, the Kubelka and Munk equation is simplified to

$$R = \frac{[(1 - R_b)S l + R_b]}{[(1 - R_b)S l + 1]} \quad (5)$$

where R is the reflectance at a medium thickness l , R_b is the back reflectance of the medium, that is, reflectance at the back glass/air interface, and S is the scattering coefficient. The magnitude of S relates to the film-scattering properties and

therefore varies with the particle size and distribution within the film. With the assumption that R_b is negligible, the equation can be further simplified to

$$R = \frac{S l}{S l + 1} \quad (6)$$

This equation is equivalent to the following equation.

$$S l = \frac{R}{T} \quad (7)$$

T is the transmittance at a medium thickness l . For a film thickness, L , of the TiO₂ film,

$$\sigma = S L = \frac{R_0}{T_0} \quad (8)$$

R_0 is the film reflectance and T_0 is the film transmittance. σ is termed the optical thickness.^{28,29} Because the optical thickness is widely accepted as an indication of the light-scattering efficiency through the medium,²⁸ it is reasonable to consider the optical thickness equivalent to the light-scattering magnitude for a series of TiO₂ films. For the calculation of the optical thickness, the light reflection losses at the air/glass and glass/TiO₂ interfaces were not corrected, and thus R_0 includes the light scattered and reflected from the TiO₂ film including the glass substrate. The essential point of eq 8 is that the light-scattering magnitude can be expressed according to the observed transmittance and reflectance spectra. In addition, the optical thickness of the film has a linear dependence on the scattering coefficient and film thickness, that is, the optical thickness changes solely with its film thickness linearly if the same TiO₂ paste is used to prepare the film.

Photocurrent Measurement. Sandwich-type solar cells with a Platinum, Pt, counter electrode and an electrolyte were used for J_{sc} measurements. The counter electrode was prepared by Pt sputtering onto the SnO₂ electrode surface. The electrolyte was prepared with modification of the method described in the literature⁵ and its content is 0.6 M dimethyl propyl imidazolium iodide, 0.05 M iodine (Wako, Japan), 0.1 M lithium iodide (Wako), and 0.5 M *tert*-butylpyridine (Aldrich) in dried acetonitrile (Kanto Chemicals, Japan). Dimethyl propyl imidazolium was synthesized by modifying the method reported by Barbe et al.¹⁰ The two electrodes are separated by a polyethylene spacer (16 or 25 μ m, PANAC Ltd., Japan). Measurements were conducted by using a Xe lamp light source simulating the AM1.5 spectrum (Wacom, WXS-80C-3) with a digital source meter (Keithley 2400). The light source spectrum was calibrated by a multi-spectroradiometer (Opto Research Corp., Japan, MSR-7000).

Results

Transparent TiO₂ films are commonly used for kinetic measurements such as charge separation and recombination in the dye-sensitized TiO₂.^{13,17,18} Optical transient measurements for the scattered films are extremely difficult because the probe light cannot quantitatively be collected owing to the light-scattering nature. Thus, it is assumed that the kinetics are identical for both transparent and scattered films, and the J_{sc} is believed to increase in proportion to the LHE increase by the addition of light-scattering (relatively large) particles into the paste. The present study facilitates the quantification of the LHE and the electron-transfer

(26) Kubelka, P.; Munk, F. *Z. Tech. Phys.* **1931**, 12, 593.

(27) Kubelka, P. *J. Opt. Soc. Am.* **1948**, 38, 448–457.

(28) Ishimaru, A. *Wave Propagation and Scattering in Random Media*; IEEE Press: New York, 1997.

(29) Mudgett, P. S.; Richards, L. W. *J. Colloid Interface Sci.* **1972**, 39, 551–567.

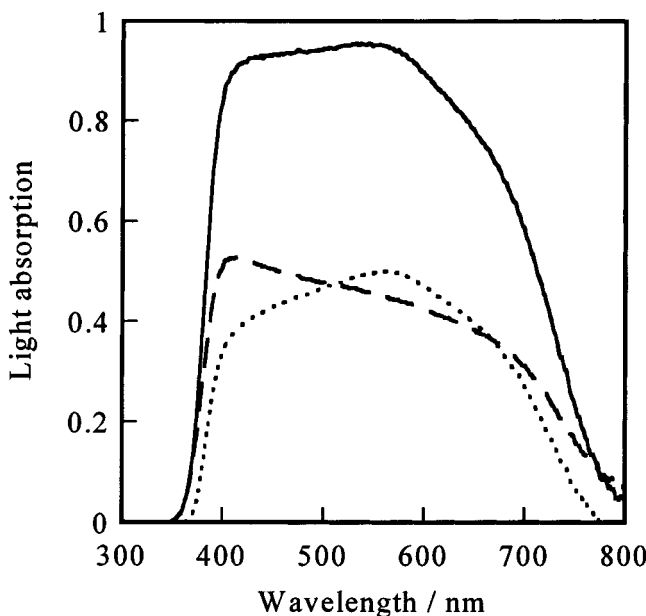


Figure 3. Ratio of absorbed photons to incident photons obtained from $Ru(dcbpy)_2(NCS)_2$ deposited onto TiO_2 (film-5). Dotted line (...) indicates the absorbed photon ratio in the backward side while the broken line (---) shows the ratio in the forward side. The total absorbed ratio (the LHE spectrum) is shown by the solid line (—). Incident light reflection at the air/glass interface is not corrected in this figure.

yield for films with a series of scattering magnitudes, and therefore the key parameters controlling the J_{sc} of the cell will be addressed.

LHE of TiO_2 Films with a Wide Variety of Scattering Magnitudes. Figure 2 shows the transmittance and reflectance spectra for film-5 (unsensitized). The proportion of reflected light increases at shorter wavelengths because the scattering efficiency is expected to be higher at shorter wavelengths. Addition of the transmittance and the reflectance spectra is also shown in Figure 2. The light collection shown by the added spectrum clearly reaches 100% at >400 nm. The scattered light loss at <400 nm can be attributed to light absorption by TiO_2 and thus the LHE in this wavelength region may result in greater errors. The transmittance and the reflectance spectra were also observed quantitatively for a series of scattered films by the integrating sphere detector (the data are not shown).

Transmittance and reflectance spectra were also measured for the identical TiO_2 films, but sensitized by the dye. The LHE was calculated by adding the absorption spectra for the forward and the backward sides for a series of TiO_2 films. Figure 3 shows the forward and backward absorption spectra for film-5 sensitized by $Ru(dcbpy)_2(NCS)_2$ and the addition of these spectra. Note that the scale of light absorption is presented as the ratio of absorbed photons to incident photons. The light absorption by the film clearly approaches unity at the wavelengths between 400 and 600 nm.

In the solar cell, TiO_2 is deposited onto a SnO_2 -conducting glass electrode. Transmittance through this electrode is less because of reflection at the air/glass and glass/ TiO_2 interfaces and light absorption by the SnO_2 electrode, if any, compared to TiO_2 films prepared on the transparent glass substrate. The incident light loss by the conducting glass must therefore be considered.

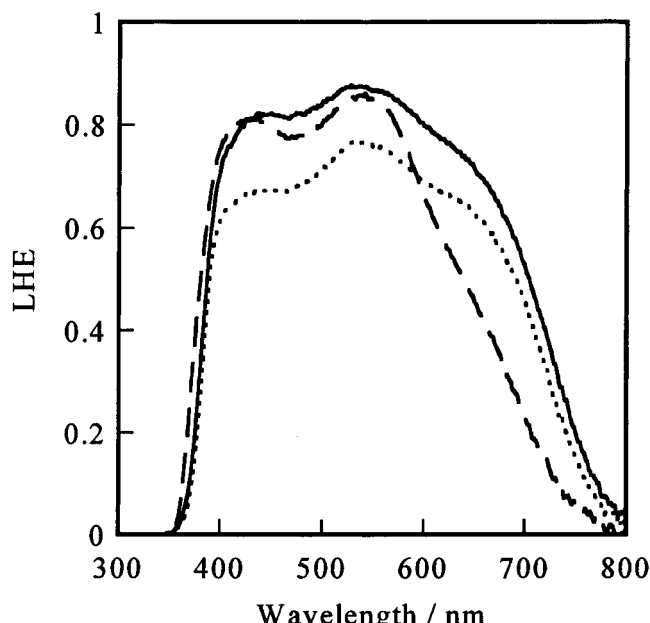


Figure 4. Spectra obtained by correcting the LHE spectra for incident light loss. Broken, solid, and dotted lines indicate spectra for film-1, -5, and -8, respectively sensitized by the dye. Light reflection at the air/glass interface in the forward side is corrected. Also corrected are light reflection and absorption by the transparent conducting glass (see Results for a detailed discussion).

After the light loss correction for the LHE spectrum shown in Figure 3, the resultant spectrum is presented in Figure 4 (solid line).³⁰ Note that there may be a contribution to the light absorption by the light confinement in the solar cell, which results from the total reflection at the glass/air interface.³¹ However, such contribution cannot currently be determined by experiment and thus the difference of the confinement in the plain and conducting glass for LHE measurements is assumed to be negligible.

Figure 4 also compares the LHE spectra of dye-sensitized TiO_2 electrodes with different light-scattering magnitudes (film-1, -5, and -8). The spectrum obtained for the transparent TiO_2 film (film-1) exhibits a similar shape to the dye absorption spectrum in the solution phase, indicating that the light absorption is essentially dominated by the concentration of the adsorbed dye within the film. The addition of relatively large particles results in the increase of the optical path length in the film; that is, light absorption by the film is enhanced at wavelengths greater than 600 nm (film-5). The excess of the large particles added in the film (film-8), however, lowers the LHE over the whole wavelength range at which the dye can absorb. In this case the total reflection loss at the TiO_2 front surface may be enhanced. This speculation is probably supported by the recent simulation result that the light absorption by the dye-sensitized TiO_2 particles near the conducting electrode

(30) Correction of the light loss was first considered for the reflection loss at the air/glass interface for the TiO_2 film deposited on the thin glass. The loss was assumed to be half of the light reflection loss by the glass (without TiO_2) covered by MeAN and another thin glass. The light loss by the conducting glass was measured individually by the integrating sphere detector (covered by MeAN and a thin glass). The loss by the conducting glass was then weighted to the LHE spectrum obtained for the dye-sensitized TiO_2 films.

(31) Usami, A. *Sol. Energy Mater. Sol. Cells* **2000**, *64*, 73–83.

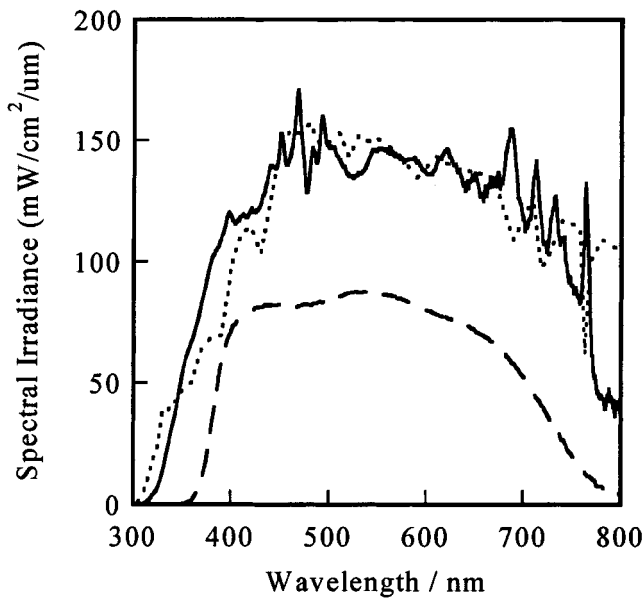


Figure 5. Comparison of spectral irradiances obtained for the light source used for the J_{sc} measurement (solid line) and taken from the literature (AM1.5 global tilt, dotted line).² The LHE (unit: percentage, broken line) taken by the dye-sensitized TiO_2 film (film-5) is also shown for the spectral overlap with the light source.

decreases, owing to the light scattering by the large particles.³¹

Electron-Transfer Yield of the Solar Cell. The cell's J_{sc} is significantly dependent upon the spectral shape and amplitude of the light source used for the measurement. It is therefore necessary to compare the light source spectrum with the standard solar spectrum to clarify the deviation from the standard. Figure 5 indicates the comparison between the observed light source spectral irradiance and the AM1.5 global tilt spectrum taken from the literature.² The corrected LHE spectrum using film-5 is also shown in Figure 5 (see Figure 4 for the corrected LHE spectrum). The total power of the light source is 99.8 mW/cm^2 in the range 280 – 2500 nm while the AM1.5 global tilt spectrum is 96.26 mW/cm^2 over 300 – 4000 nm . Within the range 300 – 800 nm at which $Ru(dcbpy)_2NCS_2$ can absorb, the maximum J_{sc} obtained from eq 1 is 25.3 mA/cm^2 for the light source used in this study and 26.1 mA/cm^2 for AM1.5 global tilt irradiance, assuming no current loss by the resistances in the cell, unity IPCE, and negligible $r(\lambda)$. Considering the light loss owing to the reflection and absorption by using the transparent conducting glass, that is, $r(\lambda) > 0$, the maximum J_{sc} is calculated to be 21.8 mA/cm^2 for the light source and 22.4 mA/cm^2 for the AM1.5 global tilt spectrum.

The average electron-transfer yield for the solar cell was calculated using eq 4. Shown in Table 2 are the J_{sc} and the calculated average electron-transfer yield obtained for various TiO_2 films. For comparison, the average electron-transfer yields using the AM1.5 global tilt spectral irradiance are also shown. The difference in film thickness for the J_{sc} and the LHE measurements were not considered as it is not possible to obtain identical film thicknesses. The calculated results in Table 2 remarkably show that the average electron transfer yield reaches nearly 100% for transparent TiO_2 films consisting of small particles. These observations

Table 2. J_{sc} , Film Thickness, Film Optical Thickness Averaged over 450 – 800 nm and Average Electron-Transfer Yields of the Solar Cell Using Two Different Spectral Irradiances (the Spectrum of the Light Source and AM1.5 Global Tilt Spectrum)^{2a}

film	J_{sc} (mA/cm ²)	film thickness: $J_{sc}/LHE (\mu\text{m})$	electron-transfer yield using light source/AM1.5 spectra	optical thickness; avg. 450–800 nm
1	13.4	10.0/9.6	1.0/0.98	0.137
2	11.4	7.9/6.9	0.94/0.91	0.313
3	11.6	8.0/6.5	0.96/0.94	0.354
4	11.1	11.2/10.8	0.82/0.79	0.750
5	13.6	8.5/8.4	0.84/0.81	0.920
6	11.5	12.3/7.8	0.76/0.74	1.16
7	9.7	15.5/14.4	0.62/0.60	1.42
8	6.7	15.0/11.7	0.48/0.47	2.03
9	4.0	6.8/6.5	0.41/0.39	2.18

^a Film thicknesses are shown for the J_{sc} and the LHE measurements, respectively.

are reproducible using synthesized or commercial particles (film-1–3). Moreover, the comparison between the transparent and scattered films reveals that the yield decreases for the scattered films. This decreasing behavior appears to follow the light-scattering magnitude (i.e., optical thickness). In these results light absorptions by the iodine electrolyte and the TiO_2 were not corrected in the calculation. These corrections may slightly alter the LHE because the photon loss by the electrolyte is generally larger in comparison to the photon absorption by the TiO_2 . For example, calculation with these corrections indicates a total LHE decrease of 5%. Contribution from the light reflection at the Pt counter electrode was not corrected because its reflectivity in the cell could not be determined.

Correlation between Electron-Transfer Yield and Optical Thickness. We now turn to an analysis of the electron-transfer yield associated with the light-scattering magnitude. Using eq 8, the optical thickness for film-5 was calculated from its transmittance and reflectance spectra. Figure 6 shows the calculated result. A sharp increase of the optical thickness at $<400 \text{ nm}$ is due to the transmittance loss by the TiO_2 absorption. This result clearly indicates that the optical thickness linearity to the scattering coefficient is wavelength-dependent. These facts hinder expressing the light-scattering magnitude of the film as one parameter. Thus, to present one parameter, the optical thickness was averaged over 450 – 800 nm and this averaging process was also applied for a series of TiO_2 films as shown in Table 2.

Comparison between the average electron-transfer yield and the average optical thickness in Table 2 clearly indicates that the average electron-transfer yield is dependent upon the light-scattering magnitude of the film. This relationship for various films is shown in Figure 7. The result shows the interesting fact that the average electron-transfer yield decreases almost linearly with the average optical thickness. The maximum difference in the electron-transfer yields reaches $\approx 60\%$ from the transparent to the highly scattered films. This must be critical to influence the J_{sc} and the solar cell performance because, in this study, the J_{sc} is essentially determined by both the LHE and the electron-transfer yield according to eq 4. The analysis was also conducted for one value of the optical thickness at 400 , 500 , 600 , or 700 nm , indicating that all the data showed an

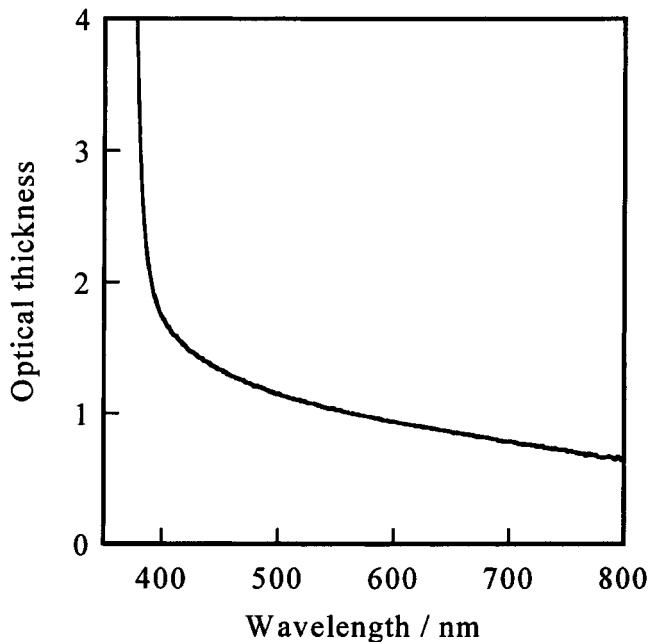


Figure 6. Wavelength-dependent optical thickness obtained for film-5. The optical thickness was obtained with the transmittance and reflectance spectra of the unsensitized film using eq 8 (see Experimental Section for the detailed calculation).

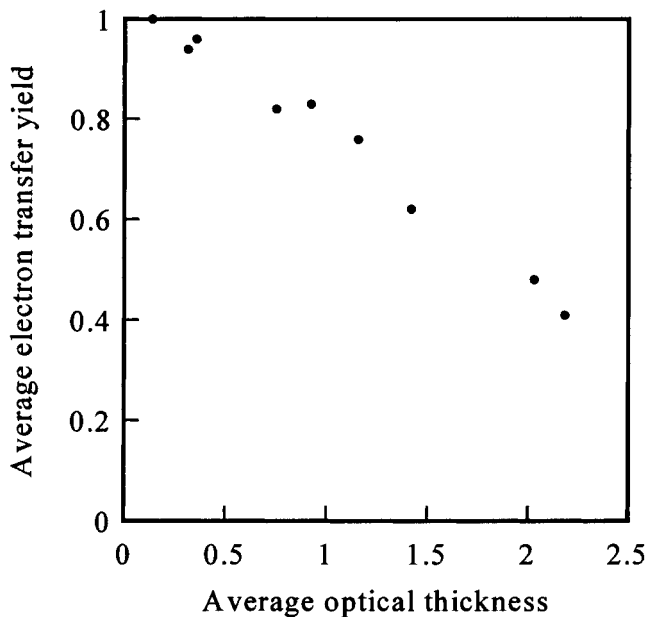


Figure 7. Average electron-transfer yield as a function of the optical thickness averaged over 450–800 nm obtained for a series of TiO_2 films.

essentially similar linear dependence upon the optical thickness at any wavelength. This fact indicates that the film-scattering property alone is independent of the wavelength. We further note that the differences in the electron-transfer yields presented in Table 2 were also compared as a function of surface area, porosity, thickness, and scattering coefficient for the films employed. None of these functions, however, showed a clear correlation with the electron-transfer yield.

Discussion

We have measured the LHE spectra for $Ru(dcbpy)_2NCS_2$ -sensitized TiO_2 films with a wide variety of light-

scattering magnitudes. With the same thickness of the TiO_2 film, the LHE was remarkably enhanced by introducing relatively large particles into the small particles, that is, increasing the light scattering, over a wide range of wavelengths (400–700 nm) as shown in Figure 4. This is attributed to the increase of optical path length (the effective distance of light path) within TiO_2 film and therefore the absorbance. However, the electron-transfer yield, that is, the product of the electron injection yield and the charge collection efficiency, decreases with an increase in the light-scattering magnitude (see Figure 7 and Table 2). This fact indicates that adding the large particles to the paste may not necessarily contribute to an improvement in the J_{sc} . Thus, the LHE at relatively longer wavelengths should be enhanced by increasing the thickness of a transparent TiO_2 film without a large loss of the electron-transfer yield to obtain the maximum J_{sc} . However, the dye extinction coefficient at wavelengths >650 nm is too small to absorb incident light only by the thickness increase. We therefore conclude that it is necessary to adjust the concentration of the large particles with appropriate size to maximize J_{sc} , considering the LHE increase and the loss of the electron-transfer yield. Its adjustment is probably dependent upon the sensitizer dye with its particular extinction coefficient.

LHE for a Wide Range of Scattered Films. In our study, large particles added into the film provide a wide variety of scattering magnitudes, enhancing the effective optical path length within the film. The LHE based upon the film sensitized by $Ru(dcbpy)_2NCS_2$ indeed increased, especially at longer wavelengths (see Figure 4). We also observed that the LHE decreased by adding an excess of the larger particles.

The LHE calculation is complex because multiple scattering properties are induced by the assembly of small and large particles. Rothenberger et al. measured scattering and absorption coefficients using transparent and scattered films and applied these parameters to estimate the wavelength-dependent LHE.¹¹ They concluded that the light absorption at relatively long wavelengths was not efficient for the transparent TiO_2 film while the highly scattered film lowered the LHE over the entire visible wavelength region. This conclusion is further supported by the results shown in Figure 4.

The experimental results in the present study reveal that the scattering coefficient is dependent upon the particle size and concentration. We therefore conclude that the maximum LHE over a wide visible wavelength range can be achieved by the appropriate size distribution and concentration of added larger particles, as was suggested by Ferber et al.¹² Our current study includes a simulation to fit the LHE obtained by the optical experiment using the optical thickness and scattering coefficient, and the results will be published elsewhere.

Dependence of the Electron-Transfer Yield upon the Light-Scattering Magnitude. The electron-transfer yield estimated in this study cannot be separated into components such as the electron injection and charge collection yields in eq 2. However, our experiments using relatively transparent films indicate an electron-transfer yield of near unity, implying that both

the injection and the charge collection yield should be near unity. This fact is consistent with the kinetic results reported previously.^{13,17}

The change in the electron-transfer yield is not obviously attributed to the change in the electron injection or the charge collection yield for light-scattering films. Owing to the use of the same anatase TiO_2 for the transparent and the scattered films, the electron diffusion length following the electron injection is expected to be identical. Thus, the charge recombination rate between an electron and an oxidized electrolyte or a dye oxidized state remains unaffected as long as the concentration of the oxidized electrolyte is balanced throughout the film. If the electron-transfer yield is lowered by decreasing the charge collection yield, it may originate from the decreased rate of the dye regeneration by the redox electrolyte. In a highly scattered medium, the light absorption is expected to be nearly complete near the light-exposed side of the TiO_2 film; that is, dye excitation is highly inhomogeneous throughout the film. Under these extreme conditions, the dye oxidized states are generated unevenly within the film and therefore the mass transport of the redox electrolyte may become a limiting step to re-reduce the dye oxidized state. The inhomogeneous concentration distribution of the oxidized electrolyte and the injected electrons in local particles within the film may, in turn, retard the dye regeneration rate and accelerate the charge recombination rate between an electron and an oxidized electrolyte, resulting in the decrease of the charge collection yield. Furthermore, this local increased number of injected electrons may raise the potential energy level by filling trap states in the particle. This increased potential level may also accelerate the charge recombination rate between the electron and the dye oxidized state in the highly scattered film because the kinetics are extremely sensitive to the excitation power or change in the electron energy level.^{23,32}

Inhomogeneous dye excitation within the highly scattered film may reduce the electron injection yield since the dye excited state or the dye oxidized state following the electron injection into TiO_2 may absorb delayed scattered light, generating effectively no electrons, that is, lowering the electron injection yield. For example, Lawandy et al. observed laser action in a dye-dissolved, highly scattered, TiO_2 colloidal solution by controlling the excitation power.³³ This study suggests that the scattered light passes through the same dye molecule in the media; that is, the dye is excited doubly or the stimulated emission is generated. However, the light source power used for the solar cells in our study is far smaller in comparison. In addition, the lifetimes of the dye excited state and the oxidized state are typically on subpicosecond and nanosecond time scales, respectively, in the cell containing the redox electrolyte.^{13,19,22} Furthermore, a recent kinetic study suggests that the electron injection kinetics is insensitive to the laser power for the transparent TiO_2 films.³⁴ It is therefore

unclear whether light absorption loss by exciting the excited state and the oxidized state may occur, thus lowering the electron-transfer yield for the highly scattered films.

The sensitizer dye, $\text{Ru}(\text{dcbpy})_2\text{NCS}_2$, commonly employed in this type of solar cell has a poor extinction coefficient over the near-infrared region (>600 nm). Increasing the optical path length by adding relatively large particles contributes to the enhanced absorption around these wavelengths. The analysis in our study supports the conclusion that the LHE in this wavelength region indeed increases using scattered films. Heimer et al. recently reported that a relatively transparent TiO_2 film sensitized by *cis*-(2,2'-bipyridyl-4,4'-dicarboxylate)₂(NCS)₂ruthenium(II) exhibits a lower electron-transfer yield (APCE) at >600 nm.³⁵ Although their experimental conditions are different from ours, this experimental result may suggest that the decrease in the electron-transfer yield for the scattered films results from the decreased electron injection yield at relatively longer wavelengths, assuming that the charge collection yield is independent of wavelength. As discussed above, the average electron-transfer yield was calculated over all wavelengths used for the light absorption, and therefore is not wavelength-dependent. Thus, to clarify this issue, a similar experimental condition to the present study, that is, using the same light source to measure the J_{sc} , must be employed to monitor the wavelength-dependent photocurrent quantitatively. This experiment is currently in progress.

Influence on Solar Cell Performance. Although the LHE increase by light scattering was theoretically described previously,^{11,12,31} experimental studies for the LHE and especially for the electron-transfer yield have to date been limited, owing to the difficulty in quantitatively capturing scattered photons emitted from the film. Moreover, it is believed that the electron injection and charge collection yields are almost unity under the short-circuit condition.^{13,19,22} We have observed that the LHE and the electron-transfer yield were remarkably influenced by introducing larger particles in the film.

We have employed various TiO_2 films prepared from our own synthesized and commercial colloids to analyze the influence of the light-scattering magnitude upon the electron-transfer yield. Within the limit of the anatase TiO_2 phase, except for film-4 (P-25, anatase:rutile = 7:3), the average electron injection yield decreases almost linearly with the optical thickness (Figure 7); that is, synthesized or commercial particles in the film exhibit an identical correlation with the electron-transfer yield. This fact suggests that there is nothing unique about using synthesized particles to prepare dye-sensitized TiO_2 films for the cell performance. Any cost-effective particles prepared by a method such as the sulfate method can therefore be employed for the solar cell fabrication. However, the drawback in using commercial particles is that they are usually agglomerated, that is, light scattering, and thus adequate mixing with different particles may be difficult for obtaining the optimum optical thickness.

If the electron-transfer yield depends solely upon the scattering magnitude, the experimental results from

(32) Nelson, J. *Phys. Rev. B—Condens. Matter* **1999**, *59*, 15374–15380.

(33) Lawandy, N. M.; Balachandran, R. M.; Gomes, A. S. L.; Sauvain, E. *Nature* **1994**, *368*, 436–438.

(34) Tachibana, Y.; Rubtsova, I. V.; Montanari, L.; Yoshihara, K.; Klug, D. R.; Durrant, J. R. *J. Photochem. Photobiol. A* **2001**, *142*, 215–220.

(35) Heimer, T. A.; Heilweil, E. J.; Bignozzi, C. A.; Meyer, G. J. *J. Phys. Chem. A* **2000**, *104*, 4256–4262.

this study suggest that the combination of a thicker transparent TiO_2 film and a sensitizer dye with reasonable extinction coefficients over a wider wavelength range, such as the panchromatic dyes presented by Nazeeruddin,⁸ would be more suitable for achieving a higher J_{sc} . Our current study involving J_{sc} measurements for this combination will be reported elsewhere. We further suggest that the methods presented in this study can be applied to search for the optimum combination of any sensitizer dye (e.g., inorganic or organic dye) and any metal oxide film (e.g., ZnO , SnO_2 , or the

mixture) and to design semiconductor films for the optimization of solar cell performance.

Acknowledgment. We are grateful to Dr. A. Usami (Central Research Institute of Electric Power Industry) for helpful discussions. We also acknowledge Mr. G. Fujihashi (Sumitomo Osaka Cement Co. Ltd., Japan) for help in synthesizing the TiO_2 colloids. This work was supported by the COE project of Science and Technology Agency of Japan.

CM011563S